Supporting Information

George et al. 10.1073/pnas.1308596110

SI Materials and Methods

Mice. *Ikbkap*$^{tm1a(KOMP)Wtsi}$ "knockout first" mice containing a *frt*-flanked *LacZ Ikbkap* reporter that disrupts the expression of inhibitor of kappa B kinase complex-associated protein or IKAP before the *LoxP*-flanked fourth exon of the *Ikbkap* gene (Fig. S1) were obtained from the International Knockout Mouse Consortium. This *Ikbkap* knockout allele was found to be homozygous lethal but *Ikbkap* expression could be rescued by removal of the β-gal cassette via Flippase-mediated recombination. The new allele contains *LoxP* sites flanking *Ikbkap* coding sequence providing the opportunity for a conditional knockout (CKO). Removal of the floxed region via Cre recombinase is predicted to yield a truncated product subject to nonsense mediated decay. To investigate the specific role of IKAP in neural crest derived tissues, we crossed homozygous *Ikbkap* CKO ($I^{C/C}$) mice to hemizygous *Wnt1-Cre* mice (Cre^{+}) carrying one copy of the conditional *Ikbkap* allele ($I^{+/C}$). For all analyses, Cre^{+}; $I^{C/C}$ embryos were used as experimental and Cre^{-} ; $I^{+/C}$ littermates were used as controls. All genotyping was performed via PCR, and primer sequences are listed below. *Wnt1-Cre* mice were purchased from The Jackson Laboratory (stock no. 003829), as well as mice bearing the *ROSA*$^{mT\text{-}mG}$ allele (stock no. 007576) (1–3). In its nonrecombined state, *ROSA*$^{mT\text{-}mG}$ causes red fluorescence in all cells. Following Cre-dependent recombination, cells convert from red to green fluorescence. All experiments with animals were performed according to the *National Institutes of Health Guide for Care and Use of Laboratory Animals* (4) and were approved by the Montana State University Institutional Animal Care and Use Committee.

Primers. *Ikbkap* CKO and wild-type (WT) alleles were distinguished using the following primers: forward (F), 5′-GCACCTTCACTCCTCAGCAT-3′; and reverse (R), 5′-AGTAGGGCCAGGAGAGAACC-3′. The presence of the Wnt1-Cre allele was detected using the following primers: F, 5′-GCCAATCTATCTGTGACGGC-3′; and R, 5′-CCTCTATCGAACAAGCATGCG-3′. The presence of the β-gal cassette was detected using the following primers: F, 5′-TTATCGATCAGCGTGGTGGTTATG-3′; and R, 5′-GTTCGGATAATGCGAACAGCGCAC-3′. Nerve growth factor (NGF) and GADPH transcript levels were compared using relative endpoint PCR and NGF primers (F, 5′- GGCATGCTGGACCCAAGCTC-3′; and R, 5′-GCGCTTGCTCCGGTGAGTCC-3′) and GADPH primers (F, 5′- GGGTGTGAACCACGAGAAATA-3′; and R, 5′- GTTGAAGTCGCAGGAGACAA-3′).

Immunohistochemistry. LacZ staining was performed as previously described (2). Apoptotic cells were identified using the In Situ Cell Death Detection Kit, TMR Red (Roche Applied Science). Immunohistochemistry was performed as previously described (5) with the addition of a 5-min incubation of slides in 1% SDS prior to the initial blocking step, to promote antigen retrieval. Microscopy images were captured using a laser-scanning confocal microscope (Olympus FV300) with 488-, 543-, and 633-nm laser lines and Fluoview software Version 5.0.

Antibodies. Primary antibodies included the following: Islet-1 (Abcam), anti-cleaved Caspase-3 (Cell Signaling), substance P (Abcam), TrkA (Louis F. Reichardt, University of California, San Francisco, CA), TrkC (R&D Systems), Runx3 (Silvia Arber, University of Basel, Switzerland), p75 NTR and Tuj-1 (Covance), p53 (Santa Cruz), phospho-histone H3 (Millipore), Pax3 (Developmental Studies Hybridoma Bank), and tyrosine hydroxylase (TH) (Millipore). Brn3A (Eric Turner, Seattle Children's Hospital, Seattle) TMR red-labeled nucleotides were amplified by immunohistochemistry with the TMR antibody (Invitrogen). For immunofluorescence, Alexa Fluor 488, 568, and 688 secondary antibodies (Invitrogen) were used. For the Western blot, tissue from embryonic day (E) 17.5 CKO and control hindbrain was homogenized, run by PAGE, and then immunoblotted with a rabbit anti-IKAP antibody (Anaspec).

Cell Counting and Statistics. Data are presented as the mean numbers of cells per section ± SEM. Every fourth section was counted with a minimum n of 3 embryos. To determine whether cell size differed between mutant and control dorsal root ganglia (DRG), TrkA^{+} somata were measured [WT, 6.68 ± 1.07 μm (n = 31); CKO, 7.09 μm ± 1.06 (n = 30); P = 0.15]. For cell counts of E17.5 DRG, ganglia from the upper lumbar region were analyzed. For counts of E12.5, E11.5, and E10.5 DRG, ganglia from the entire length of the trunk from forelimb to hind limb were analyzed. Statistical significance was determined by an unpaired Student t test and a χ^2 analysis of embryonic segregation ratios.

1. Muzumdar MD, Tasic B, Miyamichi K, Li L, Luo L (2007) A global double-fluorescent Cre reporter mouse. *Genesis* 45(9):593–605.
2. Nagy A, Gertsenstein M, Vintersten K, Behringer R (2007) Staining whole mouse embryos for {beta}-galactosidase (lacZ) activity. *CSH Protoc* 2007:pdb.prot4725.
3. Suvorova ES, et al. (2009) Cytoprotective Nrf2 pathway is induced in chronically txnrd 1-deficient hepatocytes. *PLoS ONE* 4(7):e6158.
4. Committee for the Update of the Guide for the Care and Use of Laboratory Animals (2011) *Guide for Care and Use of Laboratory Animals* (National Academies Press, Washington, DC), 8th Ed.
5. George L, Kasemeier-Kulesa J, Nelson BR, Koyano-Nakagawa N, Lefcort F (2010) Patterned assembly and neurogenesis in the chick dorsal root ganglion. *J Comp Neurol* 518(4):405–422.

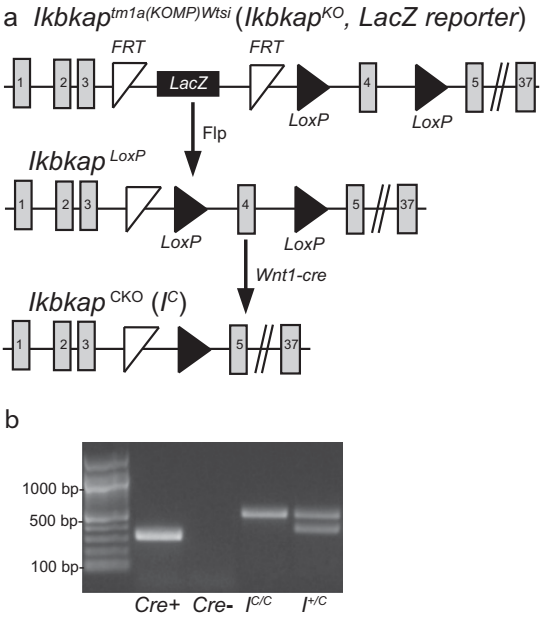

Fig. S1. Generation of *Ikbkap* CKO mice. (*A*) Schematic of conditional mutagenesis in the *Ikbkap* gene. The β-gal cassette in the knockout $Ikbkap^{tm1a(KOMP)Wtsi}$ allele, which does not express *Ikbkap*, was removed via Flippase-mediated recombination. In the new $Ikbkap^{LoxP}$ allele, *Ikbkap* is expressed, but exon 4 is flanked by *LoxP* sites (black triangles) and is excised by Cre in cells that express *Wnt1* in $Ikbkap^{LoxP/LoxP}$;*Wnt1-Cre* mice. (*B*) PCR genotyping of *Ikbkap* CKO embryos and controls. $I^{C/C}$, *Ikbkap* CKO homozygous; $I^{+/C}$, *Ikbkap* CKO heterozygous. See *SI Materials and Methods* for primer sequences.

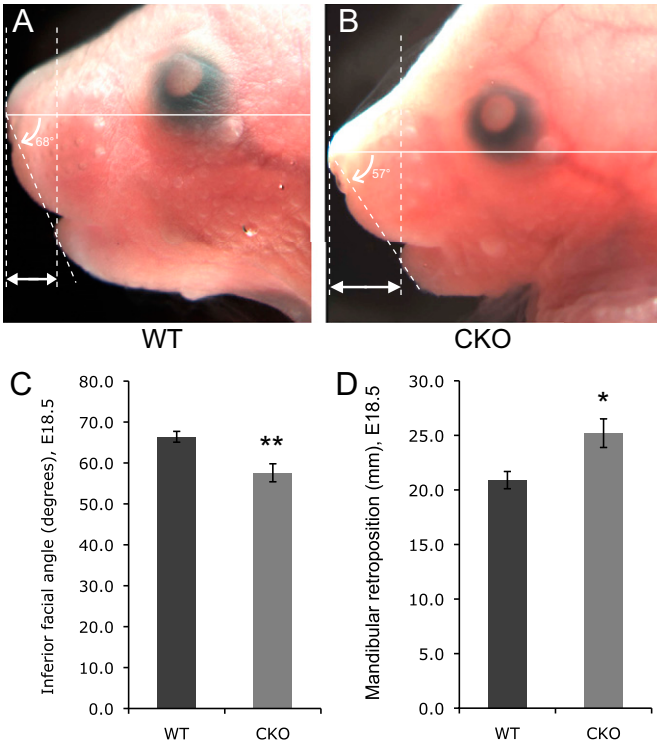

Fig. S2. *Ikbkap* CKO mice. (*A–D*) E18.5. CKO embryos exhibit a decreased inferior facial angle (*A–C*) and increased mandibular retroposition (*D* and double arrows in *A* and *B*). $*P < 0.05$; $**P < 0.01$.

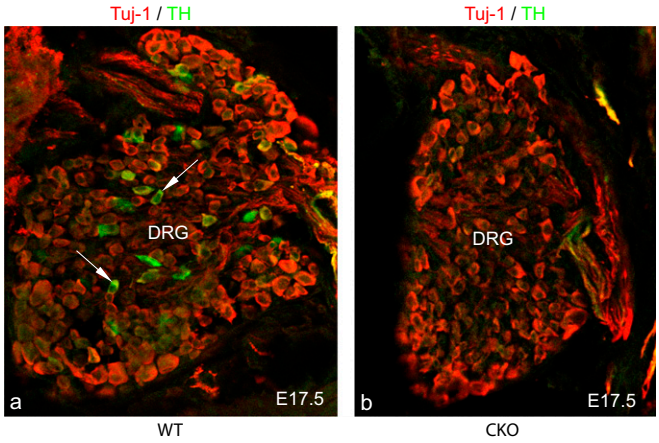

Fig. S3. TH$^+$ neurons are depleted in the CKO DRG. (*A* and *B*) Immunostaining with antibodies against TH and Tuj-1 show a dramatic reduction in the number of TH$^+$ neurons in the DRG of CKO embryos (*B*) compared with littermate controls (*A*).

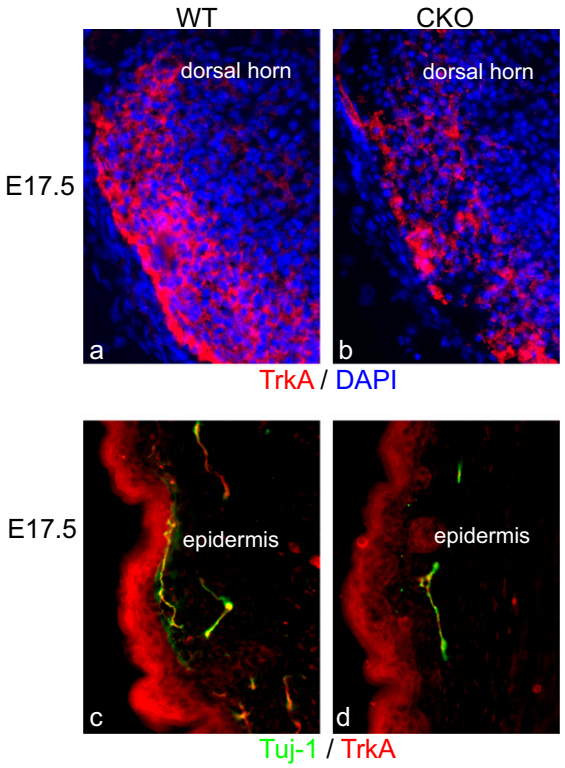

Fig. S4. TrkA$^+$ projections are reduced in *Ikbkap* CKO embryos. (*A*–*D*) E17.5. (*A* and *B*) TrkA$^+$ fibers in the dorsal horn of the spinal cord are reduced in CKO embryos (*B*) compared with controls (*A*). (*C* and *D*) TrkA$^+$ fibers in the skin are also less prevalent in mutant embryos compared with WT littermates. (Scale bar: 40 μm.)

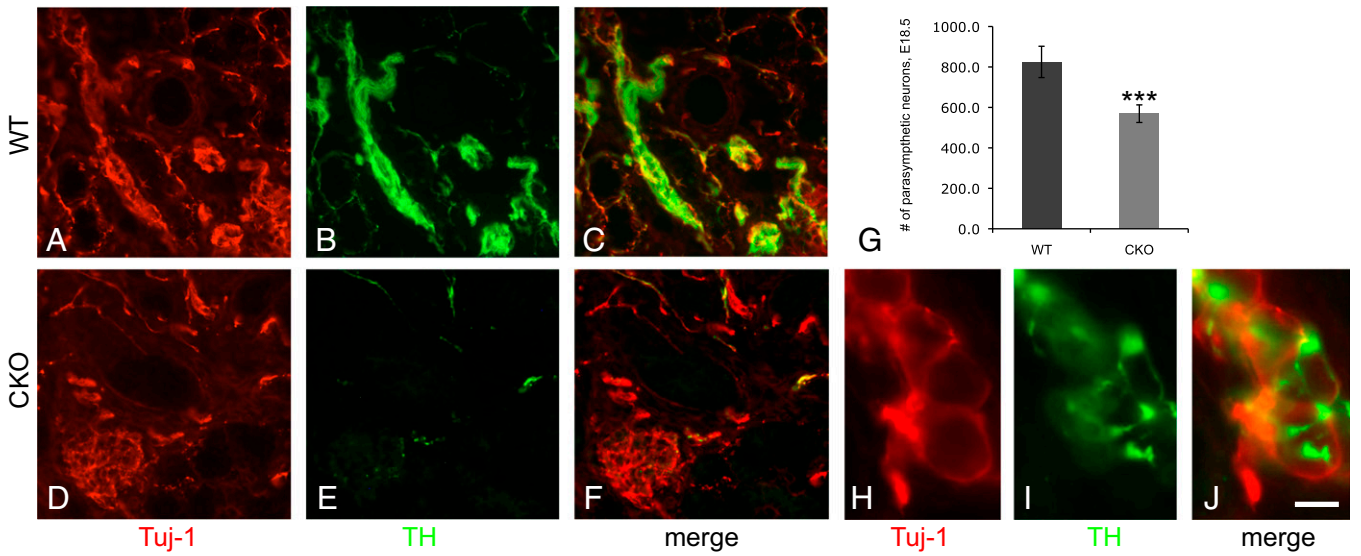

Fig. S5. Reduced sympathetic and parasympathetic innervation of the submandibular gland in *Ikbkap* CKO embryos. (*A*–*G*) The number of parasympathetic neurons in the SMG of CKO embryos is reduced (*D*–*G*) compared with littermate controls (*A*–*C*). (*H*–*J*) Parasympathetic neuronal cell bodies are heavily innervated by TH$^+$ sympathetic terminals in control embryos, whereas TH$^+$ axons are rare in the mutant SMG (*E*). (Scale bar: *A*–*F*, 50 μm; *H*–*J*, 10 μm.) ***$P < 0.001$.

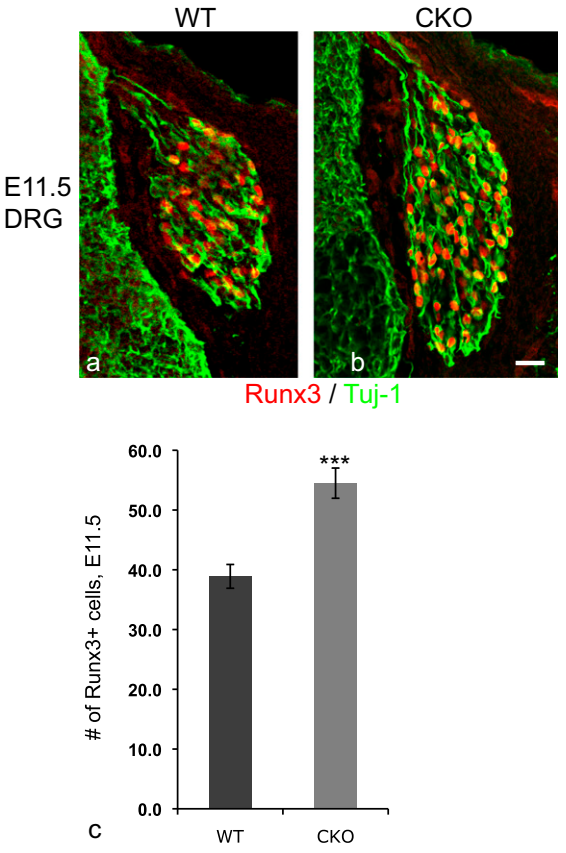

Fig. S6. The number of Runx3$^+$ neurons is increased in the DRG of *Ikbkap* CKO embryos. (*A*–*C*) At E11.5, *Ikbkap* CKO embryos show a 40% increase in the number of Runx3$^+$ neurons compared with WT controls. (Scale bar: 40 μm.)

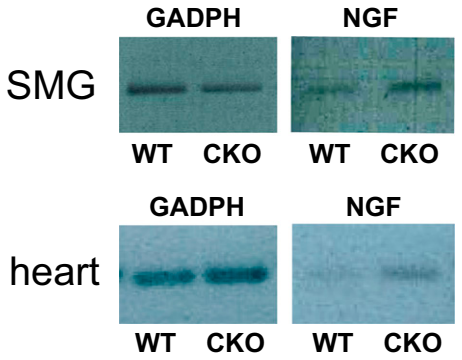

Fig. S7. The increased cell death in *Ikbkap* CKO embryos is not attributable to reduced levels of NGF. Relative endpoint PCR at E17.5/E18.5 shows that heart and submandibular gland tissues show elevated levels of NGF transcript in mutant embryos compared with controls, whereas GADPH transcript levels are the same. SMG, submandibular gland.

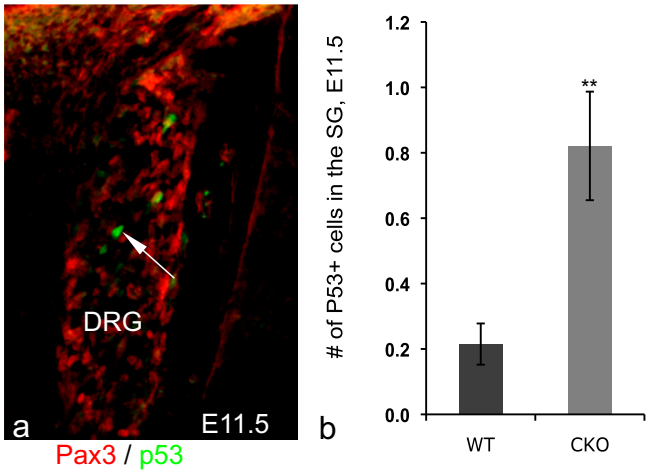

Fig. S8. The number of p53$^+$ cells is increased in the DRG and SG of *Ikbkap* CKO embryos. (*A* and *B*) At E11.5, there are significantly more p53$^+$ cells in the DRG (*A*) and SG (*B*) of *Ikbkap* CKO embryos than in WT controls. (Scale bar: 40 μm.)

Table S1. Effect of *Ikbkap* ablation on DRG development (E17.5)

Marker	Control	*IKBKAP* CKO	Difference, %	*P*
Islet	143.00 ± 7.47	96.30 ± 6.42	33↓	0.0001
TrkA	150.00 ± 6.15	80.90 ± 5.51	46↓	0.0001
TrkC	26.40 ± 1.47	30.70 ± 1.34	16↑	0.036
Substance P	4.05 ± 0.53	0.24 ± 0.07	94↓	0.001
Caspase 3	2.35 ± 0.24	5.97 ± 0.49	154↑	0.0001

All data are shown as means ± SEM. A minimum of three embryos were counted per marker. Control data were used as reference in calculating the percentage difference.

Table S2. Effect of *Ikbkap* ablation on neurogenesis

Marker	Control	*Ikbkap* CKO	Difference, %	*P*
E10.5				
Islet	71.70 ± 2.87	51.40 ± 2.60	28↓	0.0001
H3	46.40 ± 4.80	36.80 ± 6.82	21↓	0.014
Tunel	0.36 ± 0.06	0.52 ± 0.09	—	0.12
TrkA	13.4 ± 1.27	9.32 ± 0.89	30↓	0.012
TrkC	8.38 ± 0.86	7.10 ± 0.68	—	0.20
E11.5				
Islet	105.00 ± 3.52	99.80 ± 4.16	—	0.35
H3	57.70 ± 1.37	40.4 ± 1.79	30↓	0.0001
Tunel	1.72 ± 0.16	3.15 ± 0.21	83↑	0.0001
TrkA	34.80 ± 1.05	34.20 ± 1.40	—	0.40
TrkC	45.60 ± 1.75	46.90 ± 1.93	—	0.60
RunX3	38.90 ± 1.99	54.50 ± 2.53	40↑	0.0001
Pax3	146.00 ± 6.67	109.00 ± 5.00	25↓	0.0001
p53	0.14 ± 0.03	0.59 ± 0.1	321↑	0.0001
E12.5				
Islet	290.00 ± 6.79	207.00 ± 5.75	29↓	0.0001
Tunel	4.68 ± 0.51	8.08 ± 0.61	73↑	0.0001
TrkA	172.00 ± 4.03	118.00 ± 3.23	31↓	0.0001
TrkC	27.10 ± 1.76	27.00 ± 1.52	—	0.99
p53	0.26 ± 0.06	0.76 ± 0.11	192↑	0.0001

All data are shown as means ± SEM. A minimum of three embryos were counted per marker. Control data were used as reference in calculating the percentage difference. —, no significant difference.